Journal of Electronic Materials (2022) 51:3068–3077
https://doi.org/10.1007/s11664-022-09546-2

ORIGINAL RESEARCH ARTICLE

Crystal Growth of L-Alanine Oxalic Acid Crystal and its Spectral, NLO, Mechanical, Thermal, and Impedance Properties

S. Thangavel[1] · V. Kathiravan[2] · R. Ashok Kumar[1] · S. Eniya[2] · G. Satheesh Kumar[3] · P. Selvarajan[4] · M. Kumaresavanji[3]

Received: 18 December 2021 / Accepted: 22 February 2022 / Published online: 16 March 2022

Abstract

Single crystals of L-alanine oxalic acid (LAO) were grown by adopting the slow evaporation technique at room temperature. Single-crystal x-ray diffraction was used to evaluate the crystal structure of the as-grown LAO. The functional groups of LAO were identified by FT-IR spectroscopy. UV-Visible-NIR transmittance study was carried out to determine the bandgap energy. A fluorescence study was performed to obtain the emission spectrum of the LAO crystal. Vickers microhardness study was carried out to evaluate the mechanical properties of the LAO crystal. Thermogravimetric and differential thermal analysis were also conducted to investigate the thermal properties of the LAO crystal. The efficiency of the title crystal's second harmonic generation (SHG) was investigated. The electrical properties were estimated by impedance study. A laser damage threshold (LDT) study revealed that the LAO crystal has a high laser damage threshold.

Keywords X-ray diffraction · FTIR · UV · fluorescence · thermal analysis · impedance · SHG

Introduction

Organic materials are gaining research prominence due to their fascinating nonlinear optical properties in applications such as optical communication, optical computing, optical amplifiers, optical parametric oscillators, second harmonic devices, and other electro-optical devices.[1] Organic materials are immensely appealing from a technical standpoint because of their inherent nonlinearity, synthetic flexibility, high laser damage threshold, and ability to modify their characteristics via functional replacements.[2,3] Amino acids are chemical compounds composed of a proton donor carboxylic acid (COOH) and a proton acceptor amine (NH_2) group. They are utilized to synthesize novel derivatives and as a guide for the discovery of new second- and third-order NLO [nonlinear optical] materials.[4–7]

L-Alanine is the smallest chiral amino acid known in nature. It has a non-reactive hydrophobic methyl group (CH_3) as a side chain. Over a broad pH spectrum, L-alanine has the zwitterionic form (NH_3^+ and COO^-) both in crystal and in an aqueous solution. The family's simplest acentric member, L-alanine, was crystallized for the first time by Bernal and assigned to the $P2_12_12_1$ space group.[8–10] Earlier in the literature, the development and characterization of complexes of L-alanine single crystals were described.[11] Improved nonlinear optical (NLO) characteristics are expected when L-alanine is mixed with a variety of organic and inorganic acids to form new materials.[12,13]

A comparative study was performed by Urit et al.[14] on L-alaninium maleate (LAM) single crystal grown by the slow evaporation technique and by the Sankaranarayanan-Ramasamy (SR) method. An organic nonlinear optical material LAM was synthesized by Balasubramanian et al.[15] A new nonlinear optical organic single-crystal *l*-alaninium fumarate (LAF) belonging to the amino acid group was

✉ R. Ashok Kumar
rajamaniashokkumar@gmail.com

1 PG and Research Department of Physics, Thiruvalluvar Government Arts College, Periyar University, Rasipuram, Tamilnadu 637401, India

2 Crystal Growth Laboratory, PG and Research, Department of Physics, Government Arts College (Autonomous), Bharathidasan University, Karur, Tamilnadu 639005, India

3 Crystal Growth Laboratory, PG and Research, Department of Physics, National College (Autonomous), Bharathidasan University, Tiruchirappalli, Tamilnadu 620001, India

4 Department of Physics, Aditanar College of Arts and Science, Manonmaniam Sundaranar University, Tiruchendur, Tamilnadu 628216, India

grown from aqueous solution by employing a slow evaporation solution technique (SEST) by Ramachandra Raja et al.[16] Good-optical-quality bulk single crystals of NLO material L-alanine formate (L-ALF) were grown successfully by a modified SR method and characterized by Justin Raj et al.[17] Wojciechowski et al. have studied the photoinduced effects in L-alanine crystals.[18] Novel nonlinear single crystals with large second harmonic generation and efficient nonlinear optical properties have been studied, and these crystals could be used for optoelectronic and photonic applications.[19–27] Keeping various applications in mind, L-alanine was combined with oxalic acid using the slow evaporation technique to create L-alanine oxalic acid (LAO) crystals. Single-crystal x-ray diffraction (XRD), UV-visible transmission, Fourier transform infrared (FT-IR) spectral analysis, thermal analysis, microhardness measurement, and impedance analysis were performed on the generated crystal. The Kurtz–Perry powder test was also used to study the developed LAO crystal's NLO characteristics.

Experimental Procedure

Preparation and Growth

L-Alanine (LOBA, 99% purity) and oxalic acid (LOBA, 99% purity) were taken in a stoichiometric ratio of 1:1 and dissolved in double-distilled water. Saturated solution was prepared, and continuous stirring was performed at room temperature for 5 hours. This solution was then filtered in a vessel using Whatman filter paper. It took about 5 days to change the saturated solution into a supersaturated solution due to slow evaporation. In the supersaturated solution, minute crystals were initially formed after a period of 10 days. These minute crystals were used as the seed crystals for the further growth. Some good-quality seed crystals were immersed into the supersaturated solution in the growth vessel. After a growth period of 26 days, optically excellent crystals of LAO were extracted from the mother solution using the slow evaporation technique. The photograph of grown crystal of LAO is shown in Fig. 1. The crystal of LAO has high optical transparency and is colourless.

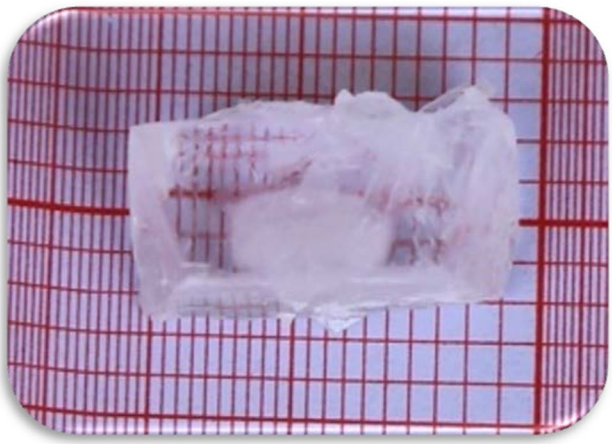

Fig. 1 As-grown crystal of LAO.

Table I Lattice parameter values of LAO crystal

Cell parameter (Å)			Volume (Å^3)	System
a	*b*	*c*	798.87	Orthorhombic
5.605	7.304	19.465		

Results and Discussion

Single-crystal X-ray Diffraction (XRD) Analysis

Using a Bruker Apex-II single-crystal x-ray diffractometer, the lattice parameters of the grown crystal were determined using single-crystal XRD analysis. This study shows that the grown crystal was an orthorhombic system with space group $P2_12_12_1$. This space group is a non-centrosymmetric space group, and hence LAO crystal has both second-order and third-order NLO properties. The values of lattice parameters are $a = 5.605$ Å, $b = 7.304$ Å, and $c = 19.465$ Å, the angles are $\alpha = 90°$, $\beta = 90°$, and $\gamma = 90°$, and the volume is $V = 798.87$ (Å^3). The lattice parameter values are given in Table I.

Fourier Transform Infrared (FT-IR) Spectral Study

A Perkin Elmer spectrometer was used to record the FT-IR spectrum in the range 4000–500 cm^{-1} at room temperature using the KBr pellet technique. Figure 2 shows the LAO crystal's recorded FT-IR spectrum.

O–H stretching causes the absorption peak to appear at 3210 cm^{-1}. C–H stretching causes the vibration peak at 2917 cm^{-1}. NH stretching is responsible for the peak at 2379 cm^{-1}. C=O symmetric stretching is responsible for the peak at 1715 cm^{-1}. The transmission peaks observed at 1581 and 1506 cm^{-1} correspond to the ammonium group (NH_3^+ bending). In the crystal, the carboxylic group appears as COOH, and an ionized carboxylic group is clearly observed in the region of 1444–1111 cm^{-1}.

The vibration peaks observed at 969 and 915 cm^{-1} are attributed to the overtone of the torsional oscillation of NH. The C–N deformation and C=O deformation mode of the vibration peak at 820 cm^{-1} are due to ring deformation. Absorption peaks characterizing different functional groups are shown in Table II.

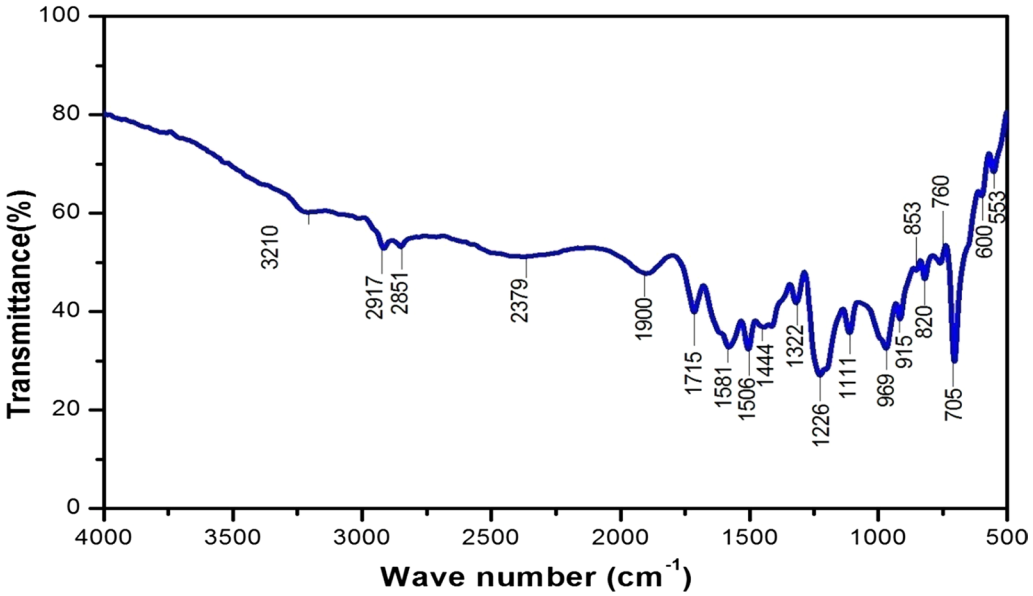

Fig. 2 FT-IR spectrum of LAO crystal.

Table II FTIR peaks and their assignments for LAO crystal

Wavenumber (cm^{-1})	Assignment
3210	O–H stretching vibrations
2917	C-H stretching
2379	NH stretching
1715	C=O symmetric stretching
1581,1506	NH bending
1444–1111	COO^- symmetric stretching
969,915	Overtone torsional oscillation of NH
853	C–C–N stretching
820	Ring deformation
760	O–C–O deformation
705	C=O deformation
600	C–N deformation
553	COO^- rocking

Optical Studies

UV-Vis-NIR Spectral Analysis

The optical transmission spectra of a well-grown LAO crystal were measured in the range 190–1100 nm using a PerkinElmer Lambda 35 spectrophotometer. The spectrum was recorded using an as-grown LAO crystal with a thickness of 3 mm. Figure 3 illustrates the UV-Vis-near-infrared (NIR) transmittance spectrum of the as-grown LAO crystal. It is observed that the transparency of the crystal is high in the visible region. Because this NLO crystal is mainly utilized in optical applications, it is critical to determine the UV transmission and lower cut-off wavelength. The LAO crystal's lower cut-off wavelength is 295 nm, and the bandgap energy was determined to be 4.2 eV using the formula $E_g = hc/\lambda$ eV. Due to its absence of absorption in the visible region, this crystal is obviously suitable for use as window material in optical equipment.

Nonlinear Optical Study

The second harmonic generation (SHG) performance of the LAO was estimated using the Kurtz and Perry Powder method. The fundamental beam was generated by a Q-Switched Nd:YAG laser with a wavelength of 1064 nm, a pulse duration of 10 ns, and a frequency repetition rate of 10 Hz.[28] It was transmitted through the powder sample. The laser beam's output, which emitted a brilliant green light (λ = 532 nm), verified the SHG behaviour. With 29 mJ/pulse input energy, the LAO crystal generated a 4.65 mV second harmonic signal, whereas the conventional potassium dihydrogen phosphate (KDP) crystal generated an 8.9 mV SHG. Consequently, the grown LAO crystal's SHG efficiency is 0.52 times that of the standard KDP crystal.

Luminescence Studies

When the electronic energy levels of solids are excited by light of a particular energy and then released as light, the phenomenon of fluorescence occurs. The fluorescence spectrum of the crystal was examined to verify the emission spectrum for that particular emitted state of the system and for decaying the components using a

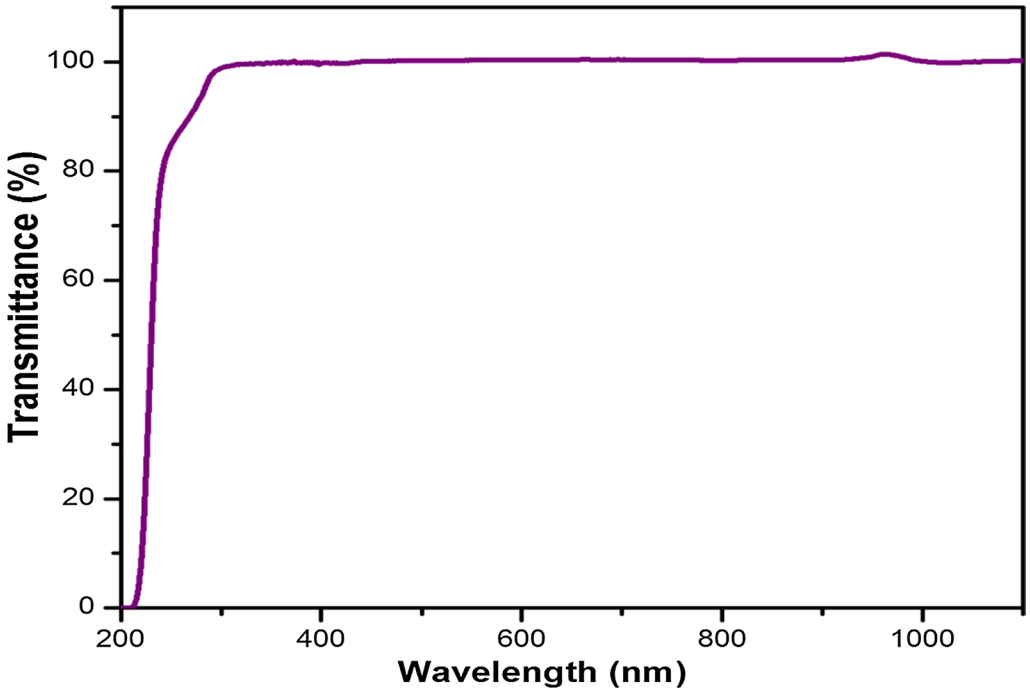

Fig. 3 UV-Vis-NIR spectrum of LAO crystal.

Perkin Elmer fluorescence spectrofluorometer, as seen in Fig. 4.[29] UV light at a wavelength of 240 nm was used as the excitation wavelength. An intense emission peak was observed around 532 nm, which is in the visible region of the electromagnetic spectrum. The result indicates that the LAO crystal has a green fluorescence emission. The title compound's powerful fluorescence emission implies that it may be a successful candidate for optoelectronic applications.[30]

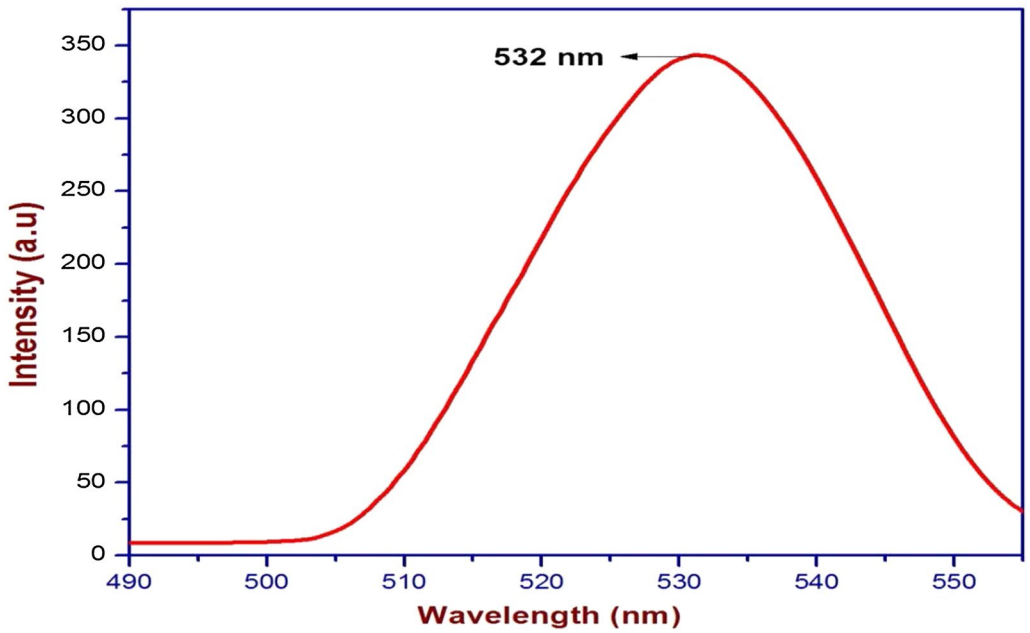

Fig. 4 Fluorescence emission spectrum of LAO crystal.

Mechanical studies

At room temperature, microhardness measurements were conducted on the flat polished face of the grown LAO crystal using a Shimadzu HMV-2T tester equipped with a Vickers diamond indenter. Using the following equation, the Vickers microhardness number (H_v) was calculated.

$$H_v = \frac{1.8544p}{d^2}\ \mathrm{kg/mm^2} \tag{1}$$

where p denotes the indenter load in kilograms and d represents the impression's diagonal length in millimetres.[31] Figure 5 illustrates the estimated load dependence of Vicker's hardness number. According to the graph, the hardness value increases as the load increases, and cracks appeared on the smooth surface of the LAO crystal above 55 g due to the release of internal stresses produced locally by indentation. The increasing trend of hardness with increase of applied load is due to reverse indentation size effect. The well-known Meyer's law $P = ad^n$, where a and d are constants that vary depending on the content, gives the relationship between load and indentation size.

The plot of log p versus log d for the LAO crystal in Fig. 6 is a straight line, and the work hardening coefficient n was determined to be 3.701. Onitsch and Hanneman previously demonstrated that the value of n is between 1 and 1.6 for hard materials and greater than 1.6 for soft materials.[32] The estimated value of $n = 3.701$ indicates that the grown LAO is soft and displays a reverse indentation size effect [RISE] (Figs. 7, 8).[33]

The yield strength (σ_y) has also been calculated from the hardness value using the relationship (for $n > 2$).[34]

$$\sigma_y = H_v/3\ \mathrm{N/m^2} \tag{2}$$

The elastic stiffness constant (C_{11}) was determined empirically using Wooster's law.[35]

$$C_{11} = \left(H_v\right)^{7/4}\ \mathrm{N/m^2} \tag{3}$$

The fracture toughness (K_c) value reflects how well the fracture resists fracture when subjected to continuous stress. The following relationship is used to determine the fracture toughness:

$$K_c = \frac{P}{\beta C^{3/2}}\mathrm{kg\ mm^{-3/2}} \tag{4}$$

where C is the crack length estimated from the middle of the indentation mark to the crack tip, and β is the indenter constant equal to 7 for the Vickers indenter.[34]

Brittleness is an inborn property that influences a material's mechanical behaviour and decides whether or not it can fracture without significant deformation. The brittleness index (B_i) value is determined using the following formula:

$$B_i = \frac{H_v}{K_c} \tag{5}$$

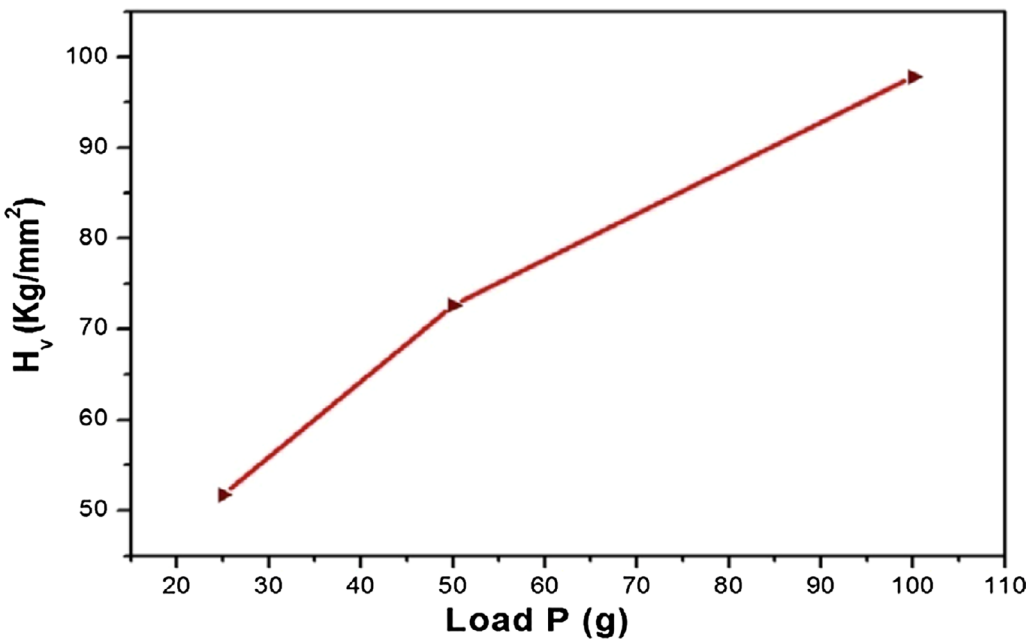

Fig. 5 Variation of Vickers hardness number with applied load for LAO crystal.

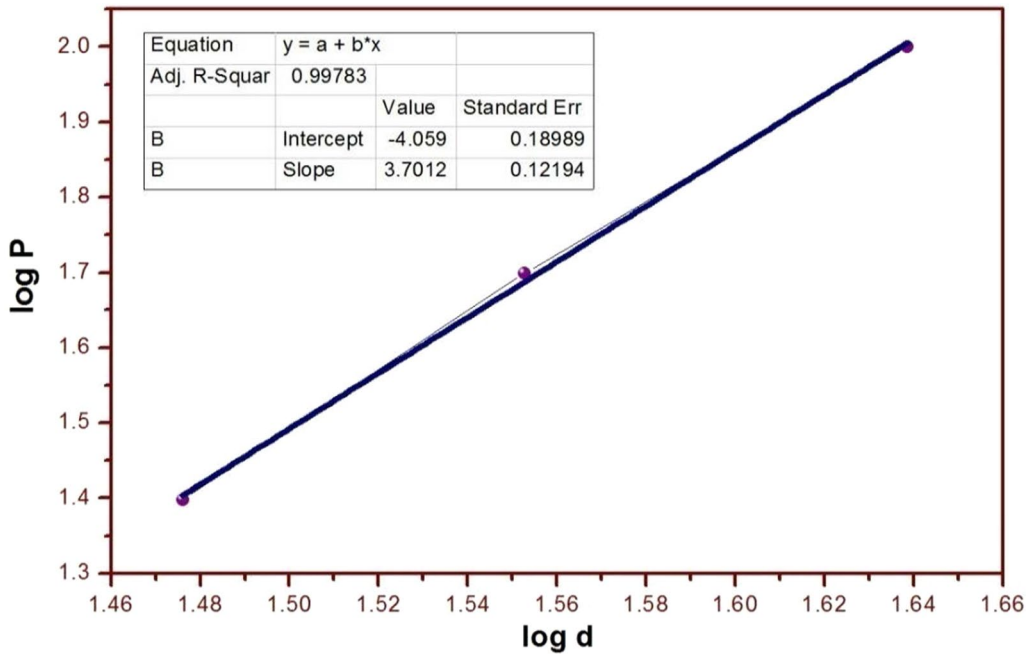

Fig. 6 Plot of log *p* versus log *d* for LAO crystal.

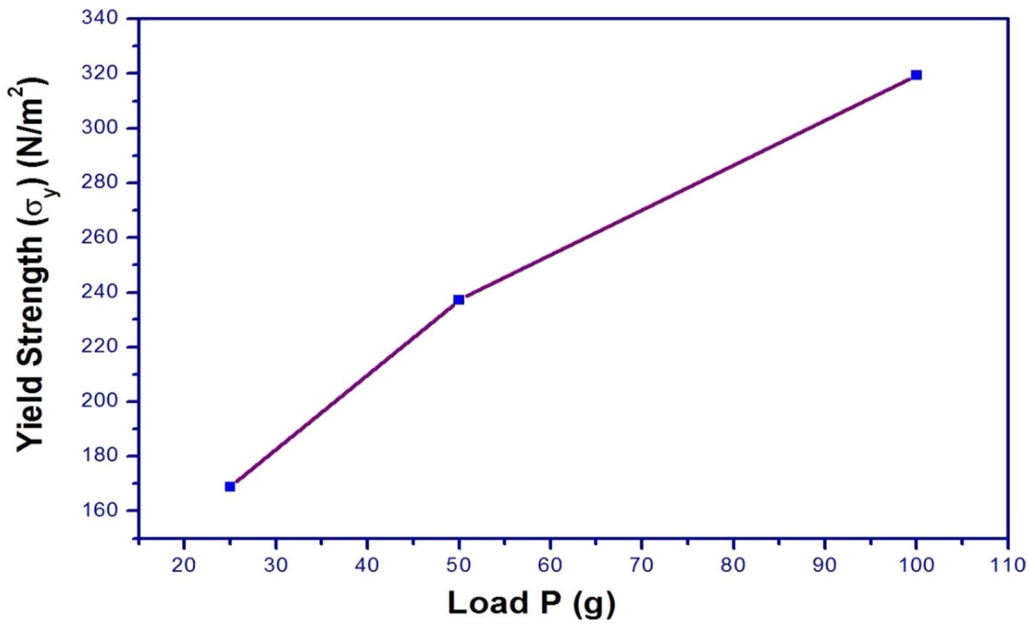

Fig. 7 Plot of yield strength versus load for LAO crystal.

The mechanical parameters like Vicker's hardness number (H_v), stiffness constant (C_{11}), yield strength (σ_y), fracture toughness (K_c) and brittleness index (B_i) are detailed in Table III for various loads (P).

Thermal Analysis—TG/DTA

Thermal analysis is a very helpful approach for characterizing a crystal's thermal stability and determining its thermal conductivity.[36] The NETZCHSTA449F3 simultaneous thermogravimetric/differential thermal analysis analyser was utilized in a nitrogen environment to conduct

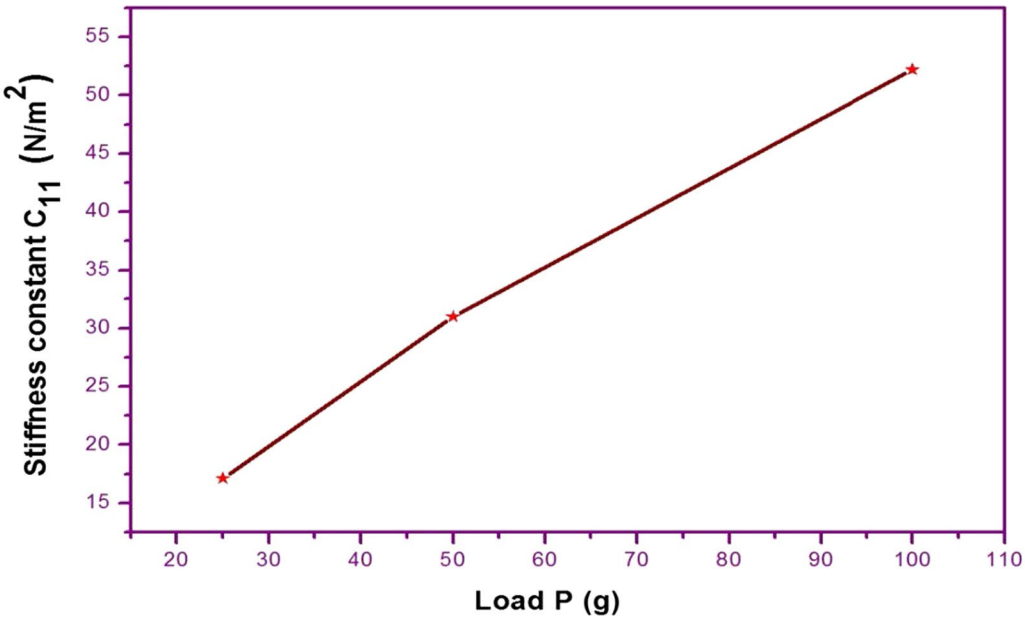

Fig. 8 Plot of stiffness constant versus load for LAO crystal.

Table III Yield strength (σ_y), stiffness constant (C_{11}), fracture toughness (k_c) and brittleness index (B_i) of LAO crystal

Load (g)	$\sigma_y \times 10^6$ N/m^2	$C_{11} \times 10^{14}$ N/m^2	K_c (kg m$^{-3/2}$)	$B_i \times 10^{-4}$
25	168.88	1.7110	1.2584	4.10
50	237.16	3.099	2.5169	2.88
100	319.48	5.2208	5.0339	1.94

thermogravimetric (TG) and differential thermal analysis (DTA) measurements in the temperature range of 27 to 1200°C at a heating rate of 10 K/min. The sample was 6.354 milligrams in weight. Figure 9 depicts the thermogram of LAO material. The TG results indicate that the loss begins at 171°C. The point of breakdown is caused by dehydration. However, no weight loss is observed between 0 and 171°C. The absence of weight loss up to 100°C verified the crystallization of LAO crystals without the presence of a water molecule. As a result, the title chemical is stable up to 171°C. Two endothermic peaks are observed on the DTA curve at 257°C and 292°C. The sharpness of these endothermic peaks indicates that the LAO crystal is a crystalline material.[37]

Impedance Analysis

The complex impedance measurement is a strong technique for determining the bulk resistance and the electrical response of a crystalline material.[38,39] The impedance spectroscopy was undertaken in order to collect the electrical features of the grown LAO crystal.[40]

Complex impedance measurement of the pellet sample was performed using a Versa STAT MC model LCR meter in the frequency range of 1 Hz to 1 MHz with the pellets held between two silver electrodes. At room temperature, it was accomplished by changing the frequency. Figure 10 illustrates the Nyquist diagram of the LAO crystal. The DC conductivity of the sample was determined using the relation

$$\sigma_{dc} = t/AR_b\ \Omega^{-1}m^{-1} \quad (6)$$

where t denotes the crystal thickness, A denotes the electrolyte's area, and R_b denotes the LAO crystal's bulk resistance. The calculated value of DC conductivity for the LAO crystal is $\sigma_{DC} = 6.536 \times 10^{-6}\ \Omega^{-1}m^{-1}$. DC conductivity values are low because charge carrier mobility decreases as ionic size decreases. The well-resolved semicircle at high frequency implies ionic conduction and the parallel combination of bulk capacitance and resistance.[41,42]

Laser Damage Threshold Study

A laser damage threshold (LDT) study was undertaken for the grown LAO crystal using a Nd:YAG laser with a wavelength of 1064 nm and 18 ns pulse width. The energy of the laser beam was measured by a Coherent energy/power meter (model no. EPM 200). The relation used to determine the LDT value is $P = E/\tau\pi r^2$ where E is the energy, τ is the pulse width, and r is the radius of the spot.[43] Laser damage involves interaction of high-power laser radiation with a crystal, and there are many processes like physical,

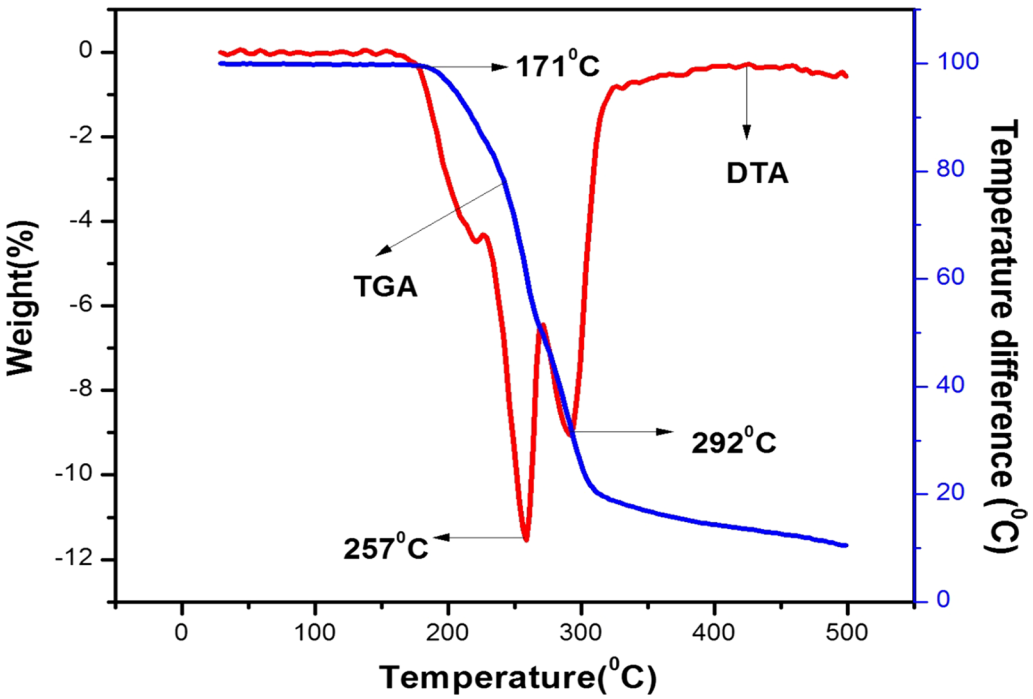

Fig. 9 TG-DTA thermogram of LAO crystal.

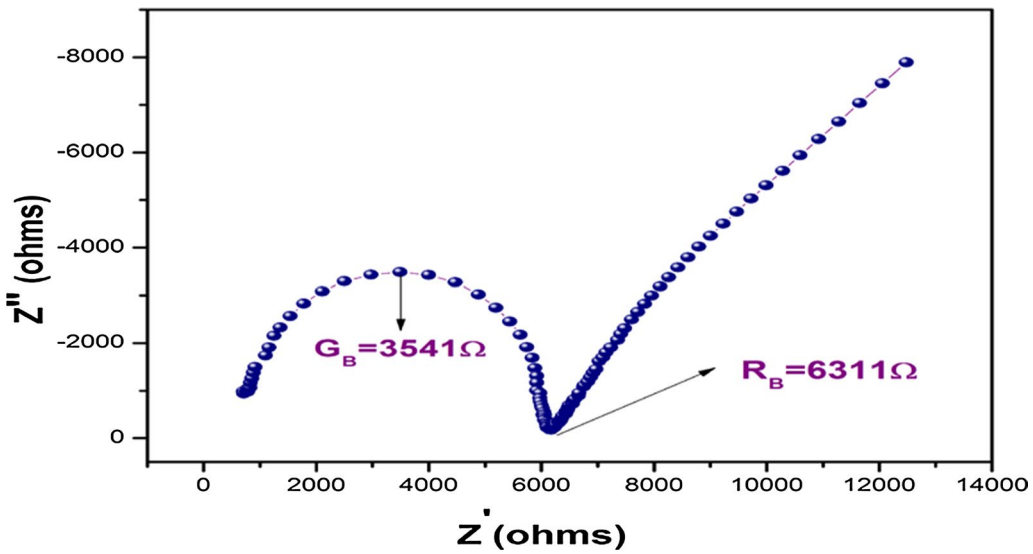

Fig. 10 Impedance spectrum of the grown LAO crystal.

chemical, optical, thermal and other processes involved. The determined value of LDT for LAO crystal is 2.492 GW/cm^2. It is observed that the LDT value of LAO crystal is greater than that of KDP (LDT value of KDP is 0.2 GW/cm^2). Since the LDT value of LAO crystal is large, this crystal could be used for NLO and laser device fabrication.

Conclusion

LAO crystals of high purity were produced using the slow evaporation solution method. The single-crystal XRD analysis indicated that the LAO crystal system is orthorhombic. FT-IR spectroscopy analysis was used to

determine the functional groups of LAO. In the UV-Vis-NIR transmittance study, the bandgap energy was found to be 4.2 eV. The fluorescence study revealed a green emission spectrum. The Vickers microhardness study was carried out to determine the hardness number (H_V), yield strength (σ_y) and stiffness constant (C_{11}), and confirmed that the LAO crystal was a soft material. Thermal stability experiments (TG/DTA) confirmed that the formed LAO crystal exhibited a reasonable degree of thermal stability up to 171°C. SHG efficiency was approximately 0.52 times that of KDP. The LDT value of the LAO crystal was found to be 2.492 GW/cm^2. Due to all of these characteristics, LAO crystals may be a viable material for nonlinear optical applications.

Acknowledgments The authors wish to express their gratitude to several research centres, including the SAIF-IIT, Madras, the ACIC-St. Joseph's College, Tiruchirappalli, the NCIF-National College, Tiruchirappalli, and Alagappa University, Karaikudi, for their contributions. The authors would like to express their gratitude to the APRC – Sacred Heart College, Tirupattur, the CIF – Pondicherry University, Pondicherry, and the IISC – Bangalore for their full-fledged assistance in carrying out the characterization measures for this research project.

Funding There is no funding involved with the current study.

Conflict of interest There is no conflict of interest in the work as declared by the authors.

References

1. Y. Mori, Y.K. Yap, T. Kamira, M. Yoshimura, and T. Sasaki, Recent development of nonlinear optical borate crystals for UV generation. *Opt. Mater.* 19, 1–5 (2002).
2. R.J. Mani, P. Selvarajan, H.A. Devadoss, and D. Shanthi, Second-order, third-order NLO and other properties of L-alanine crystals admixtured with perchloric acid (LAPA). *Optik.* 126, 213–218 (2015).
3. S. Li, K. Wu, G. Su, and Y. He, Nonlinear optical properties of some derivatives of stilbene and vinyl cyanide. *Opt. Mater.* 20, 295–299 (2002).
4. D. Shanthi, P. Selvarajan, K.K.H. Durga, and S.L.M. Ponmani, Nucleation kinetics, growth and studies of β-Alanine single crystals. *Spectro Chem. Acta Part A* 110, 1–6 (2013).
5. S. Manivannan and S. Dhanuskodi, Synthesis, crystal growth, structural and photosensitive properties of an organic NLO material. *J. Cryst. Growth* 262, 473–478 (2004).
6. J.U. Maheswari, C. Krishnan, S. Kalyanaraman, and P. Selvarajan, Characterization of potassium bromide crystals grown in the aqueous solution of picric acid. *Physica B Condens. Matter* 502, 32–38 (2016).
7. M.L. Caroline, R. Sankar, R.M. Indira, and S. Vasudevan, Growth, optical, thermal and dielectric studies of an amino acid organic nonlinear optical material: L-alanine. *Mater. Chem. Phys.* 114, 490–494 (2009).
8. A.M. Petrosyan, R.P. Sukiasyan, H.A. Karapetyan, S.S. Terzyan, and R.S. Feigelson, Growth and investigation of new nonlinear optical crystals of LAP family. *J. Cryst. Growth* 213, 103–111 (2000).
9. L. Mizoguchi, A.T. Varela, F.D. Nunes, V.S. Banat, F.F.A. Melo, J.M. Filho, and S.C. Zulia, Optical properties of L-alanine organic crystals. *Opt. Mater.* 6, 147–152 (1996).
10. P. Jayaprakash, P. Sangeetha, C.R.T. Kumari, and M.L. Caroline, Investigation on the growth, spectral, lifetime, mechanical analysis and third-order nonlinear optical studies of L-methionine admixtured D-mandelic acid single crystal: a promising material for nonlinear optical applications. *Physica B Condens. Matter* 518, 1–12 (2017).
11. J.D. Bernal, The crystal structure of the natural amino acids and related compounds. *Z. Crystallography.* 78, 363–369 (1931).
12. A.S.J.L. Rose, P. Selvarajan, and S. Perumal, Studies on growth and characterization of an NLO crystal: L-alanine hydrogen chloride (LAHC). *Mater. Chem. Phys.* 130, 950–955 (2011).
13. D. Haleshappa, B. Raghavendra, A. Jayarama, K.Q. Ching, C.K. Huey, and S.P. Parutagouda, Structural, photoluminescence, physical, optical limiting, and hirshfeld surface analysis of polymorphic chlorophenyl organic chalcone derivative for optoelectronic applications. *J. Mol. Struct.* 1232, 130053 (2021).
14. C.-I. Urit, P. Ramasamy, and P. Manyum, Comparative study on l-alaninium maleate single crystal grown by Sankaranarayanan-Ramasamy (SR) method and conventional slow evaporation solution technique. *J. Crystal Growth* 312, 2369–2375 (2010).
15. D. Balasubramanian, R. Jayavel, and P. Murgakoothan, Studies on the growth aspects of organic L-alanine maleate: a promising nonlinear optical crystal. *Nat. Sci.* 1, 216–221 (2009).
16. C.R. Raja and A.A. Joseph, Crystal growth and characterization of new nonlinear optical single crystals of L-alaninium fumarate. *Mater. Lett.* 63, 2507–2509 (2009).
17. C.J. Raj, S. Dinakaran, S. Krishnan, B.M. Boaz, R. Robert, and S.J. Das, Studies on optical, mechanical and transport properties of NLO active L-alanine formate single crystal grown by modified Sankaranarayanan-Ramasamy (SR) method. *Opt. Commun.* 281, 2285 (2008).
18. A. Wojciechowski, K. Ozga, A.H. Reshak, R. Miedzinski, I.V. Kityk, J. Berdowski, and Z. Tylczyński, Photoinduced effects in L-alanine crystals. *Mater. Lett.* 64, 1957–1959 (2010).
19. A.H. Reshak, N.M. Abbass, J. Bila, M.R. Johan, and I. Kityk, Noncentrosymmetric sulfide oxide MZnSO (M = Ca or Sr) with strongly polar structure as novel nonlinear crystals. *J. Phys. Chem. C* 123, 27172–27180 (2019).
20. A.H. Reshak, Spin-polarized second harmonic generation from the antiferromagnetic CaCoSO single crystal. *Sci. Rep.* 13, 46415 (2017).
21. A.H. Reshak and S. Auluck, The influence of oxygen vacancies on the linear and nonlinear optical properties of Pb7O(OH)3(CO3)3(BO3). *RSC Adv.* 7, 14752 (2017).
22. A.H. Reshak, Novel borate CsZn2B3O7 single crystal with large efficient second harmonic generation in deep-ultraviolet spectral range. *J. Alloy. Compd.* 722, 438–444 (2017).
23. A.H. Reshak and S. Auluck, Two haloid borate crystals with large nonlinear optical response. *Phys. Chem. Chem. Phys.* 19, 18416 (2017).
24. B.S. Naouel, O. Tarik, B. Michael, H.R. Ali, and A. Sihem, Untangling electronic, optical and bonding properties of hexagonal bismuth borate SrBi2B2O7 crystal for ultraviolet optoelectronic applications: an ab initio study. *J. Alloys Comp.* 803, 1127–1135 (2019).
25. R. Mahiaoui, T. Ouahrani, A. Chikhaoui, A. Morales-García, and A.H. Reshak, Electronic, bonding, linear, and nonlinear optical properties of Na2MGe2Q6 (M=Cd, Zn, Hg; Q=S, Se), Na2ZnSi2S6, and Na2ZnSn2S6 two metal-mixed chalcogenide compounds: insights from an ab initio study. *J. Phys. Chem. Solids* 119, 220–227 (2018).

26. A.H. Reshak, Novel ternary semiconductor CdLa2X4 (X=S or Se) single crystal with efficient second harmonic generation in the visible spectral range. *J. Alloy. Compd.* 728, 241–252 (2017).
27. A.H. Reshak, Lithium borate Li3B5O8(OH)2 with large second harmonic generation and high damage threshold in the deep-ultraviolet spectral range. *Phys. Chem. Chem. Phys.* 19, 30703–30714 (2017).
28. V. Kathiravan, G.S. Kumar, S. Pari, and P. Selvarajan, Influence of dye doping on the structural, spectral, optical, thermal, electrical, mechanical and nonlinear optical properties of L-histidine hydrofluoride dihydrate crystals. *J. Mol. Struct.* 1223, 128958 (2021).
29. S. Dhanuskodi, K. Vasantha, and P.A.A. Mary, Structural and thermal characterization of a semiorganic NLO material: L-alanine cadmium chloride. *Spectrochimica Acta Part A Mol. Biomol. Spectrosc.* 66, 637–642 (2007).
30. M. Nageshwari, P. Jayaprakash, C.R.T. Kumari, G. Vinitha, and M.L. Caroline, Growth, spectral, linear and nonlinear optical characteristics of an efficient semiorganic acentric crystal: L-valinium L-valine chloride. *Physica B Condens. Matter.* 511, 1–9 (2017).
31. D. Shanthi, P. Selvarajan, and S. Perumal, Growth, linear optical constants and photoluminescence characteristics of beta-alaninium picrate (BAP) crystals. *Optik* 127, 3192–3199 (2016).
32. M. Nageshwari, C.R.T. Kumari, P. Sangeetha, G. Vinitha, and M.L. Caroline, Third order nonlinear optical, spectral, dielectric, laser damage threshold, and photoluminescence characteristics of an efficacious semiorganic acentric crystal: L-Ornithine monohydrochloride. *Chin. J. Phys.* 56, 502–519 (2018).
33. F. Hammer, *Inorganic Chemistry* (New Delhi: Sarup Book Publishers Private Ltd., 2009).
34. M.P. Mohamed, S. Sudha, P. Jayaprakash, G. Vinitha, M. Nageshwari, P. Sangeetha, C.R.T. Kumari, and M.L. Caroline, Growth and characterization of L-histidinium fumarate fumaric acid monohydrate single crystal: a promising second and third-order nonlinear optical material. *Chin. J. Phys.* 60, 581–597 (2019).
35. S.P. Rathee and D.S. Ahlawat, Spectroscopic and thermo- electrical investigation of single crystals of L-Ornithine monohydrochloride grown by SEST. *Optik* 136, 249–258 (2017).
36. K. Meera, R. Muralidharan, A.K. Tripathi, R. Dhanasekaran, and P. Ramasamy, Growth of thiourea-doped TGS crystals and their characterisation. *J. Cryst. Growth* 260, 414–421 (2004).
37. K. Pichan, S.P. Muthu, and R. Perumalsamy, Crystal growth and characterization of third-order nonlinear optical piperazinium bis(4-hydroxybenzenesulphonate) (P4HBS) single crystal. *J. Crystal Growth* 473, 39–54 (2017).
38. Y. Le Fur, R. Masse, M.Z. Cherkaoui, and J.F. Nicoud, *Zeitschrift fur Crystallogr.* 210, 856–860 (1995).
39. M. Ram, synthesis and electrical properties of $(LiCo_{3/5}Fe_{1/5}Mn_{1/5})VO_4$ ceramics. *Solid Stated Sci.* 12, 350–354 (2010).
40. E.A. Hurtado-Aviles, M. Trejo-Valdez, J.A. Torres, C.J. Ramos-Torres, H. Martínez-Gutiérrez, and C. Torres-Torres, Photo-induced structured waves by nanostructured topological insulator Bi2Te3. *Opt. Laser Technol.* 140, 107015 (2021).
41. S. Sahoo, R.N.P. Choudhary, and B.K. Mathur, Structural, ferroelectric and Impedance spectroscopy properties of Y^{3+} modified Pb $(Fe_{0.5}\ Nb_{0.5})O_3$ ceramics. *Phys. B* 406, 1660–1664 (2011).
42. K. Ramachandran, A. Raja, V. Mohankumar, M.S. Pandian, and P. Ramasamy, Growth and characterization of 4-methyl-3-nitrobenzoic acid (4M3N) single crystal by using vertical transparent Bridgman-Stockbarger method for NLO applications. *Physica B Condens. Matter* 562, 82–93 (2019).
43. P. Vivek and P. Murugakoothan, Linear and nonlinear optical properties of a new organic NLO l-asparaginium l-tartarate (AST) single crystal. *Optik Int. J. Light Electron Opt.* 124, 3510–3513 (2013).